Petawatt laser ion acceleration with nanometer scale diamond-like carbon targets

Contact **cpalmer07@imperial.ac.uk**

C. A. J. Palmer, C. Bellei, A. E. Dangor, N. Dover, S. Kneip, S. P. D. Mangles, S. R. Nagel, Z. Najmudin, A. Rehman, and J. Schreiber
Blackett Laboratory, Imperial College London, London SW7 2BZ, UK

K. L. Lancaster, R. J. Clarke and C. Spindloe
Central Laser Facility, STFC, Rutherford Appleton Laboratory, HSIC, Didcot, Oxon OX11 0QX, UK

M. Yeung and M. Zepf
Queen's University Belfast, Belfast BT7 1NN, UK

S. Hassan and M. Tatarakis
Laboratory of Optoelectronics, Lasers and Plasma Technology, TEI Crete, 73133 Chania, Crete, Greece

S. Bott and F. Beg
Centre for Energy Research, University of California San Diego, La Jolla, California 92093, USA

A. Henig
Max-Planck-Institut für Quanten Optik, Garching, Germany

Introduction

Ion acceleration with high intensity laser pulses is a fast advancing area of research. There is a wide range of applications for controllable energetic ion beams including proton probing [1], isotope production [2] and hadron therapy [3] – a novel cancer therapy. Advancements in laser physics, specifically the development of chirped pulse amplification [4], have allowed the investigation of new acceleration regimes [5]. One such regime is that of target normal sheath acceleration (TNSA) in which hot electrons, accelerated by the laser, pass through the target and escape from the rear surface forming a strong electric field (~10^{12} V/m) at the target surface that is sufficient to ionise the rear surface atoms and accelerate the resulting ions [6]. The ion energy scaling with laser intensity for this TNSA mechanism is proportional to $(I\lambda^2)^{1/2}$ implying that at higher intensities higher energies will be achieved, however, theorists have predicted that as the laser intensity is increased beyond 10^{23} W/cm^2 a new accelerating regime can be accessed. This regime is termed radiation pressure acceleration (RPA) and exhibits much more favourable ion energy scaling with increasing intensity than TNSA (proportional to $(I\tau/\sigma)^{\alpha}$, where I is the intensity, τ is the pulse length, σ is the areal density and α is a constant equal to 2 for non-relativistic ion energies) [7].

In radiation pressure the intensity of the incident laser is sufficient to expel all the electrons from the front surface of the plasma creating a large electric field within the target, this field then accelerates the remaining ions to the same speed as the electrons so the foil is accelerated as a whole. To experimentally investigate RPA thin targets are required so that all the ions can be accelerated. The target material also needs to be strong enough to survive the laser prepulse intact. To retain a sharp density profile for the arrival of the main pulse a plasma mirror can be used to improve the contrast of the pulse. When striking a plasma mirror the prepulse will be transmitted but as the intensity increases with the arrival of the main pulse the plasma mirror will be ionized providing a reflective surface.

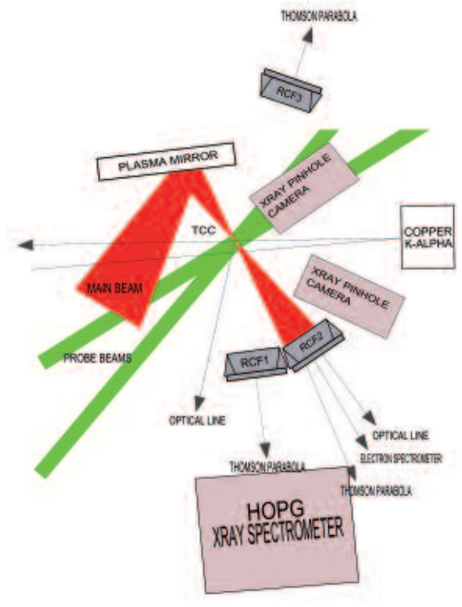

Figure 1. Schematic of ion diagnostic set up showing the positions of three stacks of radiochromic film, to measure the ion beam profile, through which holes had been cut to allow a line of sight for Thomson parabola spectrometers and other diagnostics.

Here we present measurements where diamond-like carbon (DLC) foils, with thicknesses between 5-50 nm, have been irradiated using a linearly polarised petawatt laser generating highly structured ion beams that may indicate the presence of RPA acceleration.

Experimental setup

The experiment was performed using the Vulcan Petawatt laser, a Nd:glass laser with a central wavelength of 1054 nm, based at the Rutherford Appleton Laboratory. The pulse is linearly polarised and is preceded by a 1-2 ns pedestal with a contrast of 10^{-7} to the main pulse. For the experiment this contrast was improved to 10^{-11} using a plasma mirror with anti-reflection coating. The reflectivity of the plasma mirror was measured to be 49% delivering an average energy of 296 J (σ = 7.48 J) to the target in a pulse length of 660 ± 20 fs (FWHM). During the shot on the 30 nm DLC foil the autocorrelator was suspected of failing to give an accurate pulse length, this shot has therefore not been included within the pulse length error bars. An off-axis f/3 parabolic mirror focused the beam to a spot with a diffraction limited spot diameter of 8 μm and a peak intensity of 4.7×10^{20} W/cm^2, giving a normalised vector potential $a_0 = eE/m\omega c \sim 19.6$.

Three stacks of radiochromic film (RCF), a dose dependent radiation detector, were used for each shot. RCF2 was positioned on the laser axis and RCF1 was 30° from the laser propagation direction. Both stacks were ~12 cm from the interaction point. RCF3 was 16 cm from the interaction looking at the front surface of the target at an angle of ~124° from the laser propagation direction. Each stack was made up of twelve pieces of RCF, separated by pieces of iron to allow twelve ion beam profiles for proton energies between 3-100 MeV to be detected. RCF is sensitive to laser light as well as particle radiation so a piece of aluminium foil was placed at the front of the stack to block the laser light. The pieces of metal and film within the stacks were cut such that a hole through the stack allowed the passage of ions from the interaction to three Thomson parabola (TP) spectrometers, where parallel electric and magnetic fields were used to separate the ion species and disperse the ions depending on the energies. TP2 and TP1 were ~120 cm from the interaction and aligned behind RCF2 and RCF1 respectively while TP3 was positioned ~220 cm from the interaction behind RCF3. TP1 and TP2 both used 50 μm pinholes allowing ions within a solid angle of 2.4×10^{-9} sr to enter the detector, while TP3 covered a solid angle of 58×10^{-9} sr using a 600 μm pinhole. At the rear of the spectrometers the particle tracks were detected using CR39 a plastic in which the bonds of the polymer are destroyed by the passage of particle radiation. When the CR39 plates are then etched in a concentrated (6.25 M) NaOH solution the damaged portions etch more rapidly revealing track marks which can be used to determine the incident positions of the ions. In this instance the CR39 plates were etched for 15 mins after which they were scanned before being etched again for a further 80 mins to reveal the smaller holes resulting from the passage of protons.

During the experiment four different thicknesses of DLC were used, 5 nm, 20 nm, 30 nm and 50 nm. The angle of incidence of the laser onto the target was zero degrees.

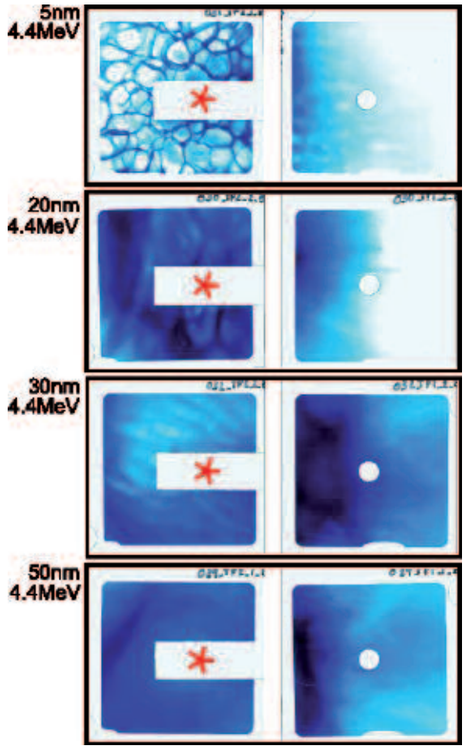

Figure 2. Radiochromic film pieces showing the 4.4 MeV ion beam profiles from RCF stacks 1, 2 for 5 nm, 20 nm, 30 nm and 50 nm DLC foil respectively. The films are placed as they would be appear looking from the interaction toward the stacks. The holes were cut to allow lines of sight for other diagnostics. The red star represents the laser axis. On arriving at the front of the stacks the laser will have diverged to a diameter ~4 cm.

Experimental results

Figure 2 shows that the ion beam profile is highly structured with the severity of the modulations decreasing with increasing target thickness. By far the most elaborate bubble pattern is visible in the beam generated from the 5 nm thick target.

On the 20 nm, 30 nm and 50 nm thick films a large, ~6 cm diameter, ring is also visible (Figure 2). Similar rings, observed in other experiments, have been explained as being the position at which the signal from the highly directional low energy ions, which are accelerated normal to the rear surface, is added to by the signal from the higher energy ions with more angled paths originating from the edge of the high intensity region at the centre of the laser focus. The bubble structure is only visible within this large ring suggesting that it originates from the central high intensity region where the laser breaks through the thin DLC foils and the central fragment, subjected to the peak intensity, is dominated by RPA.

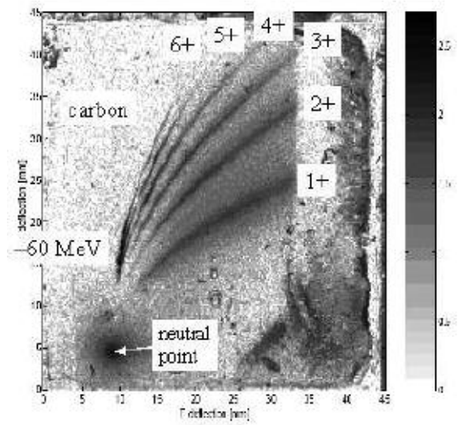

Figure 3. Scan of CR39 from the Thomson spectrometer taken after exposure to the ion beam generated from the 5 nm DLC foil and fifteen minutes etching in 6.25 M NaOH. Six different carbon charge states are visible while the proton tracks require more etching to be observed.

The results from the CR39 at the back of the Thomson spectrometer show the presence of all the carbon charge states (Figure 3). There is improved acceleration of high charge state ions and preliminary analysis suggests modulated spectra. Analysis is ongoing.

Conclusions

The presence of the bubble structure, observed on the RCF especially for the 5 nm foil shot, resembles the pattern expected for breakthrough of the foil from a highly non-linear stage of a laser-driven Rayleigh-Taylor (RT) instability – an instability which can occur at the interface between two fluids of different densities. In this case the lighter "fluid" is the light itself. When investigating RPA, using PIC simulations of a high intensity (a_0 = 34) circularly polarised pulse, Robinson et al. also observed the presence of a RT-like instability broadening their ion spectra [7]. Other simulations of RPA have also generated instabilities similar in structure to the RT instability [8,9]. The observation of the bubble structure here indicates that we have observed radiation driven effects for the first time during this experiment.

Preliminary analysis also points to anomalous ion spectra as compared to TNSA accelerated beams from thicker targets, with modulations visible at high intensities. Investigations using circularly polarized incident laser radiation may lead to further improvements in the effect of radiation drive in these experiments, and in particular may lead to the production of truly small energy spread features in the spectra of the accelerated ions.

Acknowledgements

The authors would like to acknowledge the vital assistance of the Vulcan operations team throughout this experiment.

References

1. M. Borghesi *et al.*, *Phys. Rev. Lett.* **88**, 135002 (2002).
2. P. McKenna *et al.*, *Phys. Rev. Lett.* **94**, 084801 (2005).
3. Y.I. Salamin *et al.*, *Phys. Rev. Lett.* **100**, 155004 (2008).
4. G. Mourou and D. Umstadter, *Phys. Fluids B: Plasma Physics* **4**, 2315-2325 (1992).
5. E. Clark *et al.*, *Phys. Rev. Lett.* **84**, 670 (2000), R. Snavely *et al.*, *Phys. Rev. Lett.* **85**, 2945 (2000).
6. S. C. Wilks *et al.*, *Phys. Plasmas* **8**, 542 (2001).
7. A.P.L. Robinson *et al.*, *New Journal of Physics* **10**, 013021 (2008).
8. F. Pegoraro and S. V. Bulanov, *Phys. Rev. Lett.* **99**, 065002 (2007).
9. M. Chen *et al.*, *Phys. Plasmas* **15**, 113103 (2008).